Review Articles

IJES *Iranian Journal of Earth Sciences*
Vol. 15, No. 1, 2023, 1-9.
DOI: 10.30495/ijes.2022.1968547.1800

Is skarnization the cause of mineralization? a case study, Sanandaj Sirjan zone, west Iran

Hossein Moinevaziri [1], Hossein Azizi[*2]

1. Department of Geology, Kharazmi University, Tehran, Iran
2. Department of Mining, Faculty of Engineering, University of Kurdistan, Sanandaj, Iran

Received 16 Feb 2022; accepted 3 May 2022

Abstract

The skarn type mineralization has long been accepted as an interaction of magma and the host carbonate rocks. Most researchers have considered the iron deposits in the northern Sanandaj Sirjan zone (Kurdistan area) as skarn-type mineralization which has been generated during the injection of the granitoid bodies into the host carbonate. The calculation of normative minerals from the mixed composition of granite and host dolomite shows that normal reactions cannot produce a large volume of Fe or Mn mineralization in northwest Iran as skarn deposits. One of the iron deposits which is known as the Saheb skarn deposit, 33 km east of Saqqez, NW Iran was selected for this study. The normative minerals from this deposit were calculated for a mixed composition based on 100 grams of Saheb granite and 50 grams of host dolomite. The results show the iron oxides don't extend into the last stages of magma crystallization to provide the Fe-Mn mineralization in the host rocks. Occasionally, in the contacts of plutons, various types of mineralization appear, however, they are not the result of a magma and carbonate interaction. They are probably the results of the hydrothermal fluids in the late stages of magma crystallization. The magma fluids and fossil water in the host rocks that were heated during the magma injection, leaching the Fe-Mn from the granitoid bodies and surrounding rocks. As follows, Fe-Mn-rich fluids move towards fractures and caves, finally precipitating as ore deposits into the host rocks. The skarnization phenomenon causes the reduction of volume due to the release of CO2 gas and also the crystallization of relatively dense minerals such as garnet. This process, make a partiality space for the precipitation of Fe-Mn-rich hydrothermal fluids. Our findings show that skarnization only makes space for the precipitation of the Fe from the hydrothermal fluids.

Keywords: *Skarn deposits, Hydrothermal fluids, Iron ore deposits, magma reaction, Sanandaj Sirjan zone.*

1. Introduction

Iron mineralization has largely occurred in Iran from the late Neoproterozoic up to the late Tertiary. For the mineralization of each period, a different tectonic setting such as magma differentiation, magma immiscibility, hydrothermal fluids, skarn metamorphism, and sedimentation (Haghipour 1974; Forster and Knittel 1979; Ghorbani 2013; Nabatian et al. 2015) is suggested. The mineralization of iron is mainly concentrated in the two main zones, Central Iran and Sanandaj-Sirjan (SaSZ) in western Iran (Fig 1). Most of the Iron ore deposits in central Iran are related to the magmatic activities with the Precambrian-Paleozoic ages (Haghipour 1974; Forster and Knittel 1979; Nabatian et al. 2015; Ghorbani 2013). Nonetheless, the mostly iron ore deposits in the SaSZ were controlled by Neotethys evolution from the beginning to closing. In this case, the SaSZ has been affected by the different tectonic regimes for example an extensional basin in the Paleozoic-early Mesozoic and an active margin from the Jurassic to Cretaceous (Azizi and Stern 2019; Azizi et al. 2011). Therefore, we have to consider the different types of mineralization with the different tectonic settings in the SaSZ. In the SaSZ especially in the northern part, there are a large number of small and large iron ore deposits some of which are economical (Fig1c). For example, Saqqez (Araboghli, Hassansalaran, Saheb), Marivan (Asnawa), Divandareh (Nargestala, Alijan, Tawakalan, Kanisepid, Zafarawa), Bijar (Shahrak), South Dehgolan (Meymoonawa), and east Qorveh (Galali, Khosroawa, Charmalah, Hezarkhani, Meymanatawa, and Baba-Ali). Some of them now are active mines and others are under exploration. One of them is the Saheb iron deposit 33 km east of Saqqez, NW Iran which was selected as a case study in this research. In this research, we are going to emphasize mineralization and make a clear response to why the skarnization process cannot be only the main factor for the genesis of iron ore deposits in NW Iran.

2. Geology setting and field relation

The SaSZ is a major metallogenic zone in western Iran. The SaSZ was an extensional basin that probably represents an early stage of Neo-Tethys opening from the Late Paleozoic or later, and it was an active continental margin from the Middle-late Cretaceous (Berberian, and Berberian 1981; Moinevaziri 1985; Azizi et al. 2011; Azizi and Stern 2019).

The Triassic and Jurassic sedimentary basin extended parallel to the Zagros suture zone and consisted of pellite, calcilutite, graywacke, and volcanic rocks (Berthier et al. 1974; Braud and Bellon 1974; Berberian and Berberian 1981)

---

*Corresponding author.
E-mail address (es): azizi1345@gmail.com

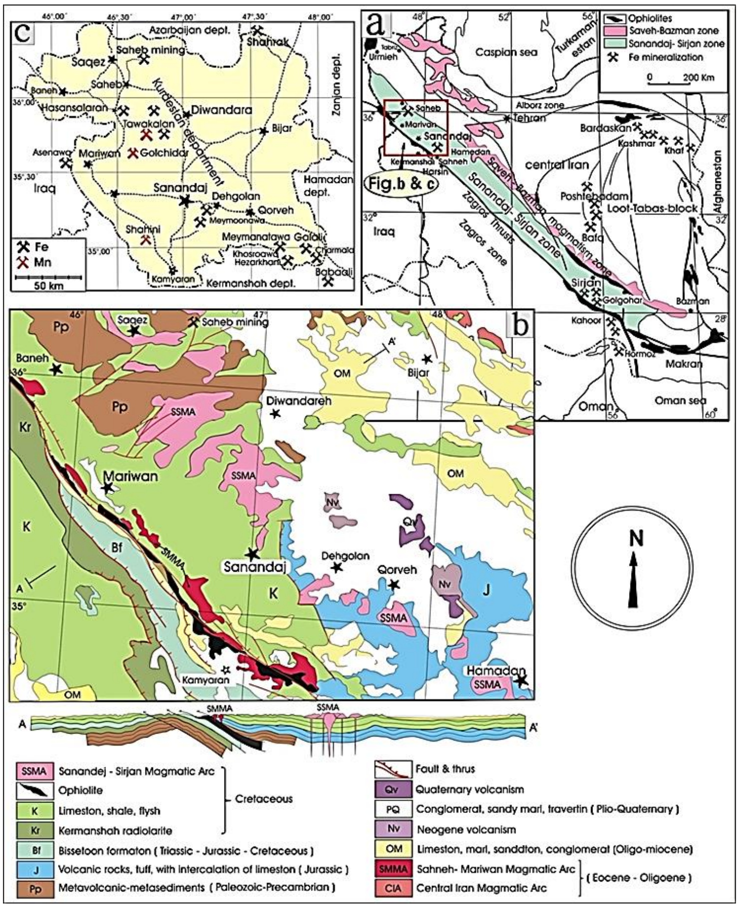

Fig 1. a) Simplified structural map of Iran (Stocklin 1968). b) Geological map of Kurdistan area, modified from 1/250,000 and 1/100,000 geological maps (Zahedi and Hajian1986; Sartipi et al. 2006); c) location map of iron and manganese mineralization in the northern SaSZ.

Sedimentary rocks were folded during the Late Jurassic orogenic phase by a weak regional metamorphic event (Mohajjel et al. 2003). A chain of intrusive bodies with a calc-alkaline signature, including diorite, quartz diorite, granodiorite to granite, and gabbroic bodies have cut the sedimentary sequences during the Late Jurassic and Cretaceous (Fig 1a). The injection of the intrusive bodies has increased the geothermal gradients in the SaSZ (Berthier et al. 1974; Massoudi et al. 2002; Baharifar et al. 2004; Ahmadi-Khalaj et al. 2007; Sepahi et al. 2014; Shahbazi et al. 2010). Multiple plutonic activities have affected the region from the Late Jurassic to Paleocene, as were reported by Valizadeh and Cantagrel (1975), Baharifar et al. (2004), Ahmadi-Khalaj et al. (2007), Shahbazi et al. (2010), Azizi et al. (2011) and Sepahi et al. (2014). The Triassic–Jurassic sequence endured a new metamorphic event related to the Laramide Orogeny at the end of the Cretaceous. Additionally, a range of calc-alkaline intrusive masses, including gabbro, diorite, and granite, intruded into the Zagros Thrust Zone (Sahneh-Marivan magmatic arc) in the Eocene-Oligocene age (Moinevaziri et al. 2008; Azizi et al. 2011). The region underwent compression phases, with faulting and thrusting, during the Tertiary. Iron mineralization in the northern SaSZ ranges in age from Precambrian to Permian, Jurassic, Cretaceous, and finally Miocene (Zahedi and Hajian 1985; Kholghi-Khasraghi 1999; Ghorbani 1993).

In most areas, iron mineralization is accommodated as interlayers within the host rocks (stratiform type). Constructive periods of stratiform Fe-mineralization were the late Neoproterozoic (Hormoz series), Permian, and Mesozoic (laterite and hematite from the Saqqez and west Divandareh). The veins of magnetite are sporadically associated with calc-silicates such as actinolite, epidote, and garnet. The presence of magnetite veins tens or hundreds of meters away from the intrusive masses and limestones excludes the possibility of a direct reaction between magma and host limestone. These observations infer that skarnization is not the main process for the geneses of ore deposits in this area.

3. Methods

In this research, in addition to the study of previous research, the following two cases have also been examined:

3.1. Field studies: more than eleven small and large iron mines and three manganese mines in Kurdistan province have been geologically studied. In this field study, the presence or absence of igneous mass and limestone in the mining area, the relationship between the deposit and the reactants (limestone and intrusive body), the presence or absence of skarn, and if skarn is present, skarn mineralogy has been studied.

3.2. Chemical-mineralogical calculation: For this calculation, the average chemical composition of some granitoid samples of the mining area is added to 50% of dolomite. After bringing the composition to 100%, skarn minerals have been calculated based on the molecular gram of oxides. In this calculation, three parageneses have been made including garnet-diopside, garnet-epidote-actinolite, and albite-epidote-actinolite.

4. Geological characteristics of iron and manganese mines in N-SaSZ

Hematite is seen in the form of laterite and sometimes pure in the Permian and Mesozoic volcano-sedimentary formations for example; Yapal and Nargestala to the west of Divandareh (Fig 2 b, c, d).

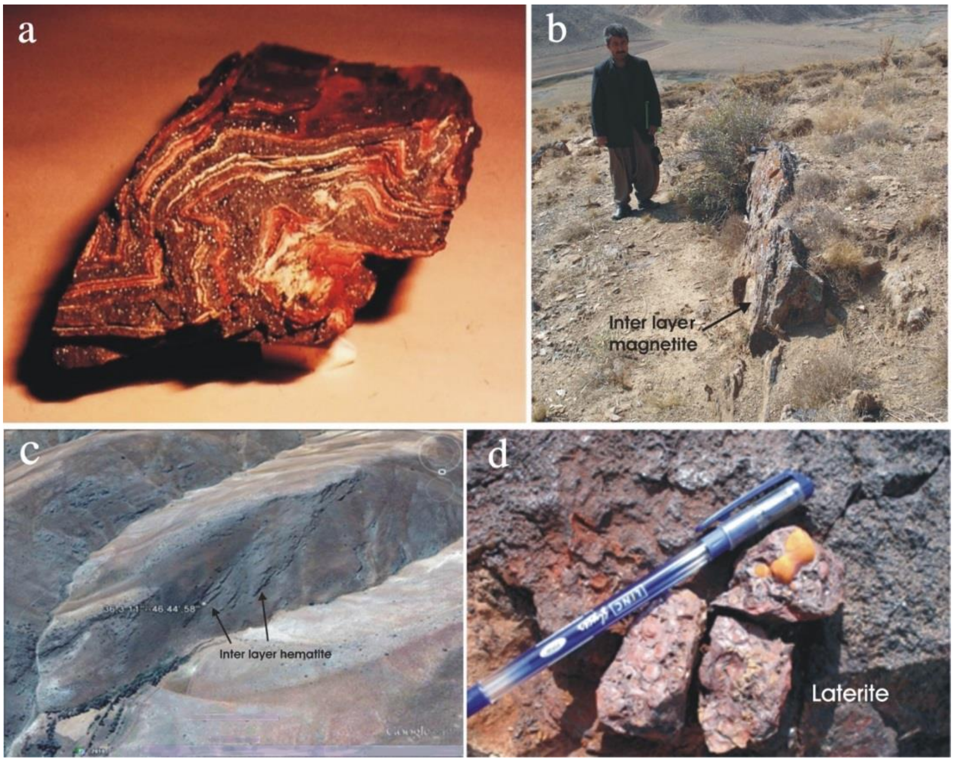

Fig 2. A) A sample of late Neoproterozoic hematite (island Hormoz, southern Iran), b) Intercalation of magnetite in volcano-sedimentary formations (Yapal, west of Divandareh), c) Sedimentary iron as laterite with minor hematite along the Jurassic- Cretaceous volcanic-sedimentary rocks (Nargestala village, east Marivan), d) Nargestala laterite. Photos b, c, and d from Moinevaziri and Mirza (2021).

Sedimentary manganese in the form of pyrolusite is found in the Bistoon group including chert, radiolarite, and volcanic tuffs, for example; Harsin (eastern Kermanshah - Fig 3a).

In the manganese mine of Tavakalan (west of Divandareh; Fig 3b), three parageneses were detected (Fig 4) which include: high temperature (spessartite and rhodonite), low oxygen fugacity (rhodochrosite and bementite) and low temperature and high oxygen fugacity (pyrolusite). While in this area, no exposure to plutonic rocks was reported. In some magnetite mines, Ca-rich silicates such as garnet, epidote, and actinolite are observed without a clear spotlight of the ingenuous rocks neither in contact nor in the iron deposits. Most magnetite and manganese deposits are situated inside the volcanic or volcano-sedimentary layers far from the plutonic massif and limestone rocks (Fig 5).

5. Calculation of normative minerals of skarn

For the normative calculation, the Saheb iron ore deposit 33 km east of Saqqez (Fig 1 b and c) was selected. According to Zandi et al. (2018), the Saheb Fe-skarn deposit was formed in the contact of the Oligo-Miocene granitoid and the Permian impure calcareous rocks. The thickness of the exo-skarn varies from 50 to 100 m (Fig 6). The mineralogical assemblage of the Saheb skarn includes garnet (andradite-grossular), clinopyroxene (diopside-hedenbergite), magnetite, and hematite (Zandi et al. 2018). For this calculation, the average chemical composition of six whole rocks of granite (Table 1) was considered and then 50% of pure dolomite (CaO = 15.2 g, MgO = 10.8 g) was added (Table 2).

Table 1. The whole rock's composition of six samples of Saheb granitoid body (Zandi et al. 2018).

sample	SiO_2	Al_2O_3	Fe_2O_3	CaO	Na_2O	K2O	MgO	TiO_2	MnO	P_2O_5	L.O.I	Total
S.2.P	70.5	14.6	2.21	2.14	4.8	3.02	1.02	0.34	0.07	0.1	1.81	99.59
S.22.P	59.03	12.8	8.95	2.09	1.03	1.01	7.12	1.59	0.17	1.15	1.56	95.51
S.11.P	56.41	14.07	6.24	5.35	3.52	2.81	4.5	1.01	0.05	0.6	0.25	9481
S.30.P	73.69	12.08	1.85	0.81	2.92	4.38	0.85	0.3	0.01	0.09	2.26	99.25
S.29.P	58.30	14.31	6.18	4.19	4.95	3.58	3.19	0.51	0.07	0.47	1.73	96.5
S.76.P	65.78	16.12	1.55	3.41	5.53	3.91	1.9	0.53	0.05	0.39	0.92	100.11

Table 2. Mean chemical composition of 6 samples of Saheb granitoid Data from Zandi et al. 2018). 50 g of dolomite (CaO = 15.2 g, MgO = 10.8 g) were added to 100 grams of granitoid and then normalized to 100%. Fe2O3 converted to FeO in this study based on FeO = Fe_2O_3* X 0.9.

	SiO_2	Al_2O_3	Fe_2O_3	CaO	Na_2O	K_2O	MgO	TiO_2	MnO	P_2O_5	L.O.I.	Total
Average of granitoid	63.95	14.0	4.5	3.0	3.79	3.12	3.1	0.71	0.07	0.47	1.42	97.63
				15.2			10.8					
Granite + dolomite	63.95	14.0	3.26 (FeO)	18.2	3.79	3.12	13.9	0.71	0.07	0.47		121.47
%	52.64	11.52	2.68	14.98	3.12	2.56	11.44	0.58	0.06	0.38		99.98

After mixings and normalized to 100, the normative minerals were calculated based on the mixed composition. In this calculation, three skarn parageneses have been made including garnet-diopside (Table 3), garnet-epidote-actinolite (Table 4), and albite-epidote-actinolite (Table 5). The normative minerals from the three types of skarns paragenesis show that the reaction between granitic magma and the host carbonate does not lead to the release of iron oxides deposit.

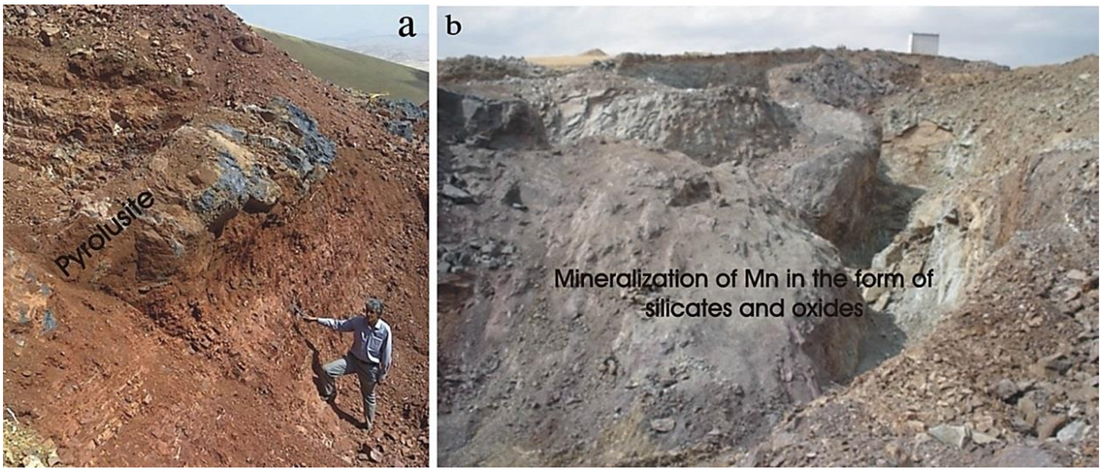

Fig 3. a; Sedimentary interlayered manganese deposits (pyrolusite) with radiolarite, chert, and acidic volcanic tuffs (Harsin and Kermanshah area), b: high and low-temperature hydrothermal deposit of manganese (Tavakalan, west of Divandareh).

6. Discussion

Iron mineralization in the northern SaSZ ranges in age from Precambrian to Permian, Jurassic, Cretaceous, and finally Miocene. Magnetite veins are sometimes associated with calc-silicate minerals such as actinolite, epidote, and garnet.

These deposits were the topic for many researchers with different purposes on the genesis. For example, Kazemirad (2010) states the Fe-Mn deposits of Heneshk, Goli, and Cheshme-Esi of the southeastern part of SaSZ are considered with a volcano-sedimentary origin and are related to Triassic magmatism by extension. Babaki and Aftabi (2006) proposed that the iron in Golghar deposits originated from the seawater during the leaching of older rocks in the oceanic rift and finally precipitated as the silicate and exhalative hydrothermal fluids. Nabatian et al. (2015) suggested that the development of volcano-sedimentary deposits of Fe and Fe-Mn in the SaSZ and Zagros is compatible with an extensional environment. Tavakoli (2003) and Motavalli (2004) declare the magnetite deposits of Baba-Ali, Galali, Chenar-olia, and Tekyaebala in the southeast Kurdistan area (Fig 1, c) are related to Triassic-Jurassic volcano-sedimentary rocks in a rift basin.

Motavalli (2004) suggested four stages of Fe mineralization in this area as follows; 1. Precipitation of iron deposits in the volcano-sedimentary sequences of the Jurassic rift basin. 2. Folding, deformation, and metamorphism near the greenschist facies. 3. In this stage, the magmatic injection made contact metamorphism and skarn-type mineralization in the host carbonates. 4. Development of shear zones and concentrated iron in the fractures. Therefore, Hamekasi, Khosro-Abad, and Galali Iron deposits as skarn-type mineralization have been generated during the early to late Jurassic (Motavalli 2004).

Table 3. Calculation of garnet, and diopside paragenesis based on the data in Table 2.

		SiO_2	Al_2O_3	FeO	CaO	Na_2O	K_2O	MgO	TiO_2	MnO	P_2O_5	Number of minerals milli-molecules	Molecular weight	% Normative minerals of skarn	
Oxides milli molecules		877	113	37	267	50	26	282	7	1	2				
Apatite	P_2O_5, 3CaO				255						0	2	310	0.62	
Ilmenite	TiO_2 , FeO			30					0			7	152	1.06	
Garnet	$3SiO_2$ Al_2O_3 3CaO	658	40		36							73	450	39.42	
	$3SiO_2$, Al_2O_3, 3MgO	568	10					192				30	402	12.06	% Garnet 56.46
	$3SiO_2$ Al_2O_3 3FeO	538	0	0								10	498	4.98	
Diopside	$2SiO_2$	310													
	MgO							0				192	100	19.20	% CPX
	CaO				0							36	116	4.17	23.37
Magnetite	Fe_3O_4											0		0	
Quartz	SiO_2											310	60	18.60	
Total														100.11	

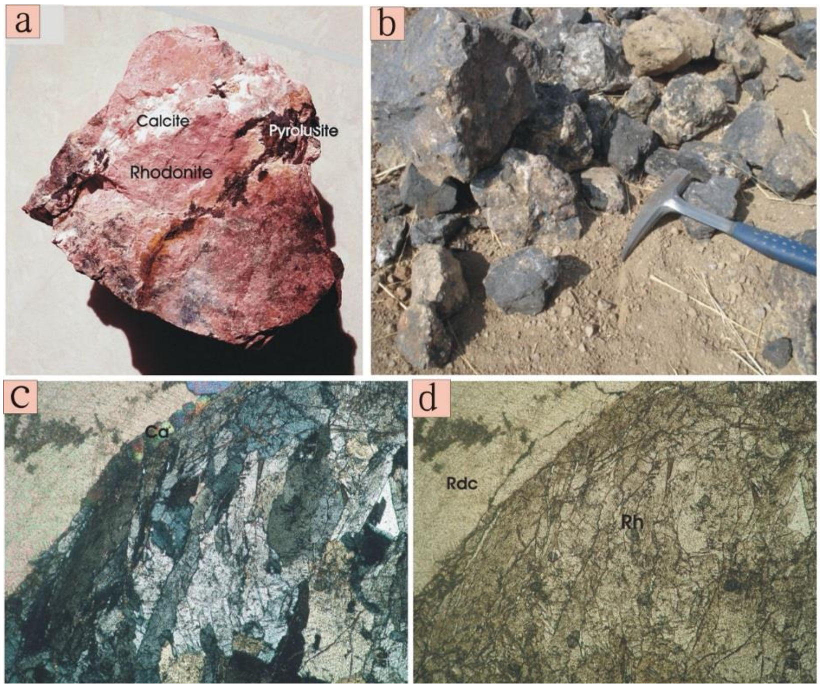

Fig 4. a) Manganese ore deposits from the Tavakalan mine (west of Divandareh) include rhodonite, pyrolusite, and calcite. b) Pyrolusite in the Tavakalan. c, and d) Photographic image of rhodonite with XPL (cross-polarized light) and PPL, respectively.

Table 4. Calculation of garnet, epidote, and actinolite paragenesis based on the data in Table 2.

		SiO_2	Al_2O_3	FeO	CaO	Na_2O	K_2O	MgO	TiO_2	MnO	P_2O_5	Number of minerals milli-molecules	Molecular Weight	% Normative minerals of skarn
% Oxides (mixture)		52.64	11.52	2.68	14.98	3.12	2.56	11.44	0.58	0.06	0.38			
Oxides milli molecules		877	113	37	267	50	26	282	7	1	2			
Apatite	P_2O_5, 3CaO				255						0	2	310	0.70
Ilmenite	TiO_2 , FeO			30					0			7	152	1.21
Garnet	$3SiO_2$ Al_2O_3 3CaO	802	88		180							25	450	12.85
	$3SiO_2$, Al_2O_3, 3MgO	742	68					222				20	402	9.18
	$3SiO_2$ Al_2O_3 3FeO	712	58	0								10	498	5.69
Epidote	$3Al_2O_3$ 4CaO $6SiO_2$	474	0		105							19	890	19.32
Actinolite-Tremolite	$4SiO_2$, CaO, 3MgO,	178			32			0				74	416	35.17
Magnetite	Fe_3O_4											0		0
Calcite	CO_3 Ca				0							32	100	3.65
Quartz	SiO_2	0										178	60	12.20
Total	99.97													

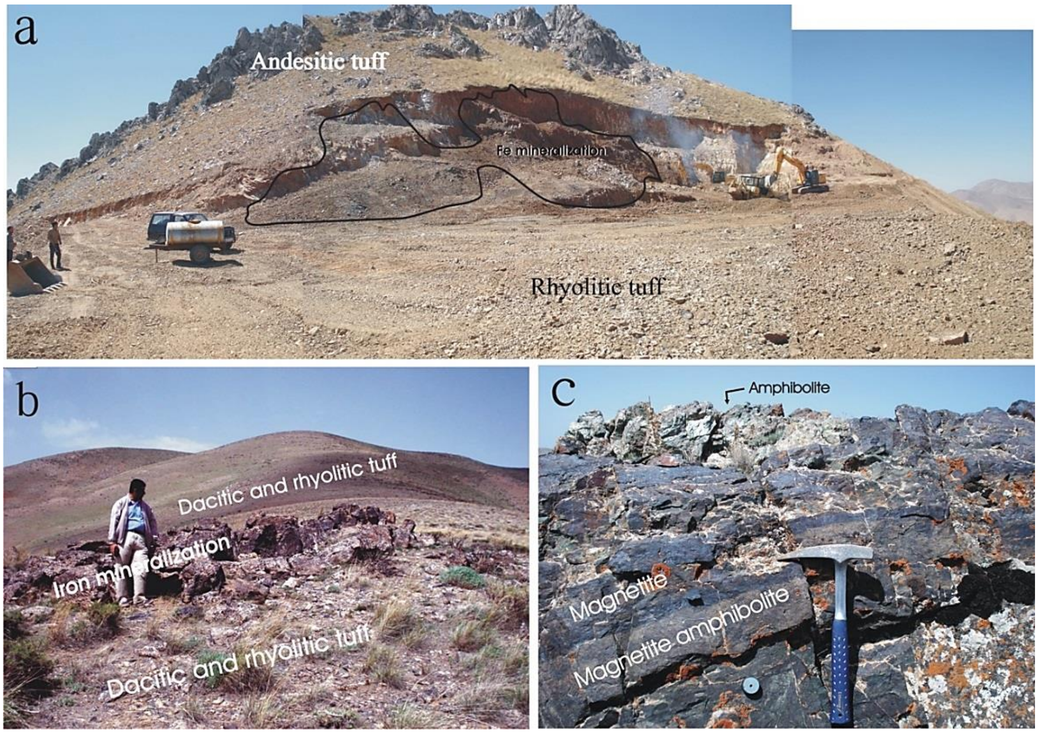

Fig 5. The presence of the magnetite deposit in the volcanic rocks without limestone. a) East of Qorveh (South of Galali), b) South of Dehgolan (Meymoonabad), magnetite veins cut the rhyolitic and dacitic tuffs. c) Magnetite as an interlayer in the Jurassic meta-basalt and meta-tuff. The photos from Moinevaziri and Mirza (2021)

Baghban et al. (2021) have discussed the formation of numerous cracks in the Saheb skarn zone, which have caused the iron-bearing hydrothermal fluids to inject the fractures, and as a result, isolated iron deposits were formed in the skarn zone. This proposal is consistent with what has been accomplished in this research. Nonetheless, in spite of that, we suggest that the source of iron is hot iron-rich water extracted from the old iron-bearing rocks and it is transferred to the cavities and fractures in the skarn zone.Based on the principles of petrography and petrology, if magma crystallizes regularly without any contamination or event minor contamination with the host carbonate (rocks poor in iron), cannot produce an economical iron deposit in any cases (Tables 1 to 5). Based on the principles of petrogenesis and the history of mineralization in this area (existence of prior sedimentary sources to feed the later hydrothermal phases) a model is presented for iron and manganese mineralization in the northern SaSZ. According to this model, apart from Late Neoproterozoic iron-rich sedimentary rocks such as the Hormoz series, some Permian and Mesozoic sedimentary rocks also contain iron and manganese oxides (Fig 7a).

Table 5. Calculation of albite, epidote, and actinolite paragenesis based on the data in Table 2.

		SiO_2	Al_2O_3	FeO	CaO		Na_2O	K_2O	MgO	TiO_2	MnO	P_2O_5	Number of minerals milli-molecules	Molecular weight	% Normative minerals of skarn
Oxide milli molecules		877	113	37	267		50	26	282	7	1	2			
Apatite	P_2O_5, 3CaO				255							0	2	310	0.62
Ilmenite	TiO_2, FeO			30						0			7	152	1.06
Albite	$6SiO_2$ Al_2O_3 $(Na,K)_2O$	421	37				0	0					76	534	40.58
Epidote	$3Al_2O_3$ 4CaO $6SiO_2$	396	0		238								12.3	890	10.94
Actinolite	$4SiO_2$ CaO 3(MgO,FeO)	0		0	144				0				104	416	43.26
Magnetite	Fe_3O_4	0											0		0
Calcite	$CaCO_3$				0								45	100	4.5
Total															100.96

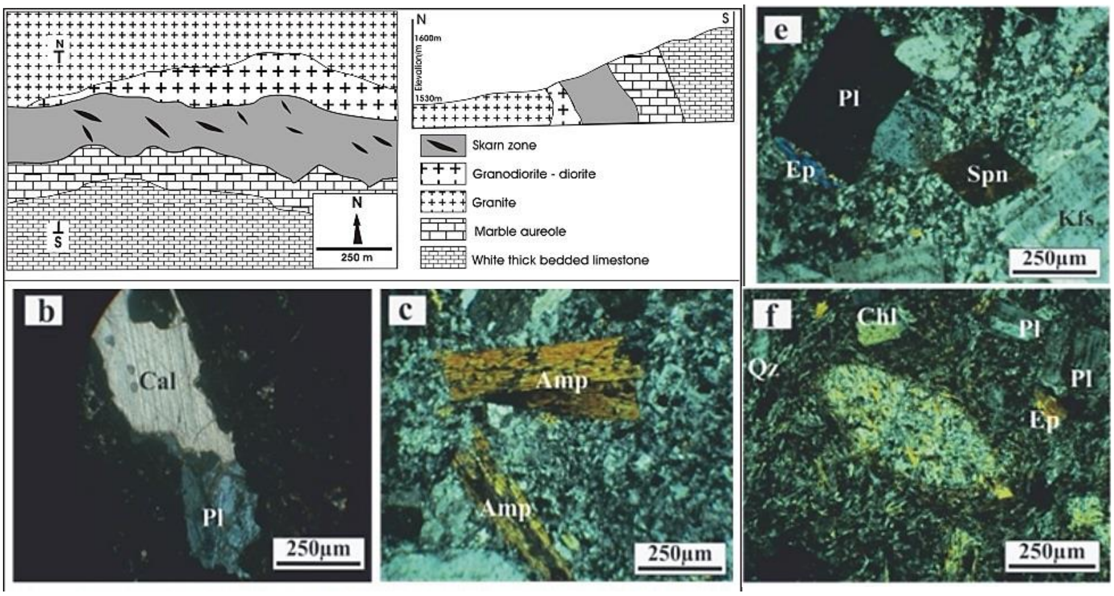

Fig 6. Geological map of the Saheb iron deposit with1:5000 scale (Zandi et al. 2018). b-f: Microscopic images of non-metallic minerals observed in Saheb skarn (Zandi et al. 2018). These are volcanic rocks, not skarn.

The injection of plutonic bodies during the Mesozoic and Tertiary relocated the Fe-Mn from the sedimentary rocks and transported them near the surface (Fig 7b). During this process, Sedimentary hematite (Fe^{3+}) and pyrolusite (Mn^{4+}) under the influence of lower oxygen fugacity were changed to Fe^{2+} and Mn^{2+} as the following silicate minerals such as garnet and rhodonite, were precipitated. During the increase of oxygen fugacity due to the interference of the meteoric water (Fig 7c), Fe^{2+} and Mn^{2+} change to Fe^{3+} and Mn^{4+} and it is favorable to the crystallization of magnetite and pyrolusite. Due to the escape of CO_2 during the skarnization, a large volume of limestone is reduced. In addition, high molecular volume minerals will be replaced by high-density minerals such as garnet. Therefore, in the phenomenon of skarnization, a large volume of free space appears and it would be favorable for the migrant of the hot fluids and precipitation of their components.

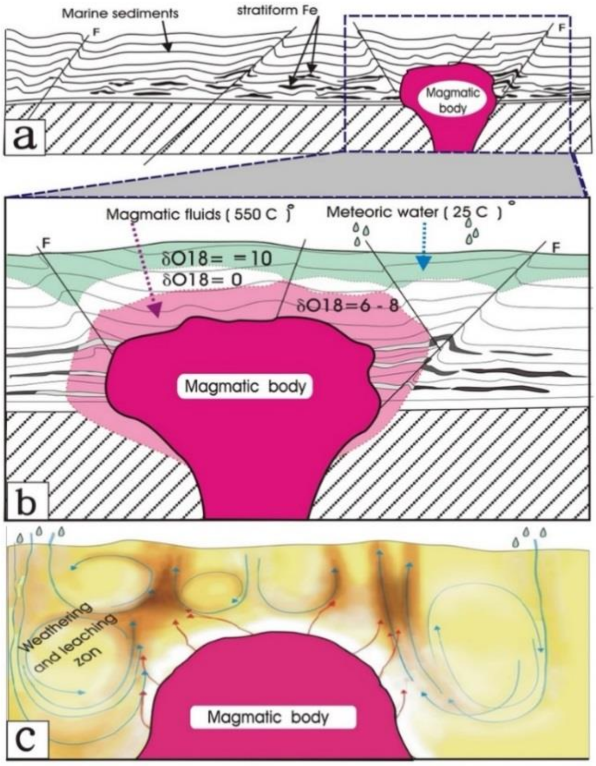

Fig 7. a) Precipitation of the iron and manganese oxides in the sedimentary basins during the Late Paleozoic to the early Cretaceous. b) Injection of the intrusive bodies increases the geothermal gradient, as the following release the fluids from the surrounding rocks. c) The circulation, combination, and convection of the fluids released from the intrusive bodies and hot meteoric water leaching the Fe-Mn from the earlier rocks and finally precipitation of that in the faults and surface fractures.

7. Conclusion

The basement sedimentary rocks in the northern SaSZ have some Fe-Mn-rich interlayers. These layers can be a large feeding for iron and manganese deposits during the circulation of hot water. Hot fluids carry the Fe and Mn from the earlier rocks and under the control of lithostatic pressure, temperature, oxygen fugacity, pH, etc., different types of minerals such as silicates, carbonates, sulfurs, or oxides will be precipitated. Our normative calculation based on the mixed composition of the granite and carbonate shows that the skarn processes will not lead to the release of iron oxides and probably no other oxide deposits. Actually, after the decarbonization of skarn, the released fluids from the magma and also hot fluids from the aureole of intrusive bodies, solve, wash and carry the Fe and Mn to the shallow depths. The materials from the fluids will be principiated at low temperature in the cavities and fractures which have been created during the skarnization. This research shows that the recycling of Fe and Mn from the host rocks can be considered the main mechanism for the generation of the SaSZ iron and manganese deposits instead of the skarnization that was previously suggested.

Acknowledgments

In this research, the data from Zandi et al. (2018) were used, so we feel it is our duty to thank them. We also thank Dr. Dabiri for handling this paper.

References

Ahmadi-Khalaj A, Esmaeily D, Valizadeh MV, Rahimpour-Bonab H (2007) Petrology and Geochemistry of the Granitoid Complex of Boroujerd, Sanandaj-Sirjan Zone, Western Iran, *Journal of Asian Earth Sciences* 29: 859-877.

Azizi H, Asaharab Y, Mehrabi B, Chungd SL (2011) Geochronological and geochemical constraints on the petrogenesis of high-K granite from the Suffi abad Area, Sanandaj-Sirjan Zone, NW Iran, *Chemie der Erde* 71(4): 363-376.

Azizi H, Stern RJ (2019) Jurassic igneous rocks of the central Sanandaj–Sirjan zone (Iran), mark a propagating continental rift, not a magmatic arc, *Terra Nova* 31(5): 415–423.

Babaki A. Aftabi A J (2006) Investigation on the Model of Iron Mineralization at Gol Gohar Iron Deposit, Sirjan-Kerman, *Geosciences Scientific Quarterly Journal* 61: 40-59 (in Persian).

Baghban S, Zandi Z, Lentz D (2021) Formation and evolution of the calcic-magnesian Saheb Fe (Cu) skarn deposit from the Sanandaj-Sirjan Belt, NW Iran: Evidence for multistage boiling in episodes of magnetite saturation, *Journal of Geochemical exploration* 226: 106781.

Baharifar AA, Moinevaziri H, BellonH, Piqué A (2004) The crystalline complexes of Hamadan (Sanandaj-Sirjan zone, western Iran): metasedimentary Mesozoic sequences affected by Late Cretaceous tectono-metamorphic and plutonic events, *Comptes Rendus Geoscience* 336(16): 1443-1452.

Berberian F, Berberian M (1981) Tectono-plutonic episodes in Iran, Zagros, Hindu Kush, *Himalaya Geodynamic Evolution* 3; 5- 32.

Berthier F, Billault JP, Halbronn B Maurizot P (1974) Etudestratigraphique, petrologique et structural de la region de Korramabad (Zagros, Iran), Doctoral dissertation, Université de Grenoble 282 p.

Braud J, Bellon H (1971) Donnees nouvelles sur le demaine metamorphique du Zagros (zone de Sanandah-Sirjan) au niveau de Kermanshah- Hamadan (Iran): nature age et interpretation des séries métamorphiques et des ihtrusions: evolution structurale, *Rapport Universite Paris- Sud*: 1-20.

Förster H, Knittel U (1979) Petrographic observations on a magnetite deposit at Mishdovan, central Iran, *Economic Geology* 74(6):1485-9.

Ghorbani M (1993) Metallogeny of Iran iron deposits. Unpublished Internal Report, Shahid Beheshti University, Tehran, Iran.

Ghorbani M (2013) The economic geology of Iran, Mineral deposits and natural resources, Springer 1-450.

Haghipour A (1974) Etude géologique de la région de Biabanak-Bafq (Iran central): Pétrologie et tectonique du socle précambrien et de sa couverture, Doctoral dissertation, Université Scientifique et Médicale de Grenoble.

Kazemirad M (2010) Mineralogy, geometry, geochemistry and genesis of Heneshk, Goli and Cheshmeh Esi FeMn deposits in the northeast Safa Shahr (Fars Province), Unpublished M.Sc. thesis, Tarbiat Modares University, Tehran, Iran, 225 p.

Massoudi F, Yardley BWD, Cliff RA (2002) Rb-Sr geochronology of pegmatites, plutonic rocks and a hornfels in the region southwest of Arak, Iran. *Journal of sciences, Islamic Republicof Iran* 13(3): 249-254.

Mohajjel M, Fergusson CL, Sahandi MR (2003) Cretaceous–Tertiary convergence and continental collision, Sanandaj-Sirjan Zone, Western Iran, *Journal of Asian Earth Sciences* 21: 397- 412.

Moinevaziri H (1985) Magmatisme tértiaire et quatérnaire en Iran. Thèse d' Éta. Université Paris-Sud, Orsay, 260 p.

Moinevaziri H (2019) Manganese mine of Tawakalan in Kurdistan - Iran: A rare Mn mineralization process, *Iranian Society of Crystallography and Mineralogy* 27(2): 411-422.

Moinevaziri H, Azizi H, Mehrabi B, Izadi F (2008) Oligocene magmatism in the Zagros Thrust Zone (Sahneh- Marivan area): Evidence for the Neotethyan subduction occurrence in the Paleogene, Journal of sciences, *Tehran University* 34(1): 113-122 (in persan).

Moinevaziri H, Mirza T (2021) Characteritics and origin of iron mineralization in northern Sanandaj- Sirjan zone (Iran- Iraq). *Iraqi Bulletin of Geology and Mining* 17: 43-58.

Motavalli K (2004) Mineralogy, geochemistry and genesis of Khosro Abad and Tekye Bala iron deposits in the northeast Songhor. Unpublished M.Sc thesis, Tarbiat Modares University, Tehran, Iran, 210 p.

Nabatian GH, Rastad E, Neubauer F, Honarmand M, Ghaderi M (2015) Iron and Fe- Mn mineralization in Iran: implications for Tethyan metallogeny, *Australian Journal of Earth Sciences* 62(2): 21-241.

Sartipi AH, Haghfarshi E, Sahandi MR (2006) Geological quadrangle map of Sanandaj, 1/100000, Geological Survey and Mineral exploration of Iran.

Sepahi AA, Shahbazi H, Siebel W, Ranin, A (2014) Geochronology of plutonic rocks from the Sanandaj-Sirjan zone, Iran, and new zircon and titanite U-Th-Pb ages for granitoid from the Marivan pluton, *Geochronolometria* 41(3): 207-215.

Shabazi S (2010) Mineralogy, geochemistry and genesis of Bashkand iron deposit, southwest of Soltanieh. Unpublished M.Sc. thesis, Tarbiat Modares University, Tehran, Iran, 220 p.

Stocklin J (1968) Structural history and tectonics of Iran: a review, *AAPG bulletin* 52(7):1229-1258.

Tavakoli (2003) Mineralogy, geochemistry and source of iron deposits NW of Hamedan. Unpublished M.Sc. thesis, Tarbiat Modares University, Tehran, Iran, 157 p.

Valizadeh MV, Cantagrel JM (1975) Premieres donnees radiometriques (K-Ar et Rb-Sr) sur les micas du complexe magmatique du mont Alvand, pres de Hamadan (Iran occidental), 281:1083-1086.

Zahedi M, Hajian J (1985) Geological quadrangle map of Sanandaj 1/250000. Geological Survey & Mineral exploration of Iran.

Zandi Z, Jafrirad A, Gourabjeripour A, Lotfi M, (2018) Mineralization, Mineralogy, and Geochemistry of Saheb Fe-Cu Deposit of Saqqez (Kurdistan), NW Iran. *Open Journal of Geology* 31(8): 514-528.